Effect of Manganese and Nitrogen on the Solidification Mode in Austenitic Stainless Steel Welds

N. SUUTALA

The macrostructures and microstructures of thirty different austenitic stainless welds alloyed with manganese and/or nitrogen are analyzed. Comparison of the results with those obtained from normal welds of the AISI/AWS 300 series indicates that the solidification mode and Ferrite Number can be predicted adequately using chromium and nickel equivalents. The solidification mode in the normal and nitrogen-alloyed welds can be best described by the equivalents developed by Hammar and Svensson and the Ferrite Number by the conventional Schaeffler-DeLong diagram. Both of these descriptions are invalid at high manganese content values (5 to 8 pct), however, in which case Hull's equivalents give a better correlation between the composition and the solidification mode or Ferrite Number. The complicated role of manganese and the austenite-favoring effect of nitrogen in austenitic stainless steels are discussed.

I. INTRODUCTION

MANGANESE and nitrogen are interesting alloying elements in austenitic stainless steels in many respects. Apart from its conventional use for deoxidation and sulfide control at contents of 1 to 2 pct, manganese is also added, often with nitrogen, as a substitute for the expensive element, nickel. Alloys containing 4 to 10 pct Mn and 0.05 to 0.30 pct N (*e.g.*, AISI 200 series) have been developed in this manner. On the other hand, a modified AISI 316 steel containing only about 0.15 pct Mn has also been designed in order to increase resistance against pitting corrosion.[1] Nitrogen alloying considerably improves the strength of austenitic stainless steel, and it is claimed that nitrogen also increases resistance to pitting corrosion.[2]

A higher amount of manganese is also added in certain weld filler metals for austenitic stainless steels, the best-known types being perhaps 18Cr-8Ni-6Mn, 18Cr-16Ni-6Mn-3Mo, and 20Cr-25Mn-5Ni-2Mo. This alloying is mainly done in order to improve resistance to solidification cracking and fissuring in fully austenitic welds.[3,4,5] The mechanism of this beneficial effect, and the whole role of manganese, are uncertain as far as the solidification and the transformation from ferrite to austenite are concerned. At low contents, manganese is generally regarded as an austenite former,[6–12] whereas at higher contents it is thought to favor ferrite.[4,8,10,14] This discrepancy is also reflected in different manganese coefficients in nickel equivalents (Table I). As seen in this table, the interstitial solutes carbon and nitrogen are also those elements whose coefficients seem to vary markedly. It is thus possible that the coefficients of these elements may be dependent both on the content of the element concerned, and on the overall composition and the temperature.

Brooks[15] has stated that the ferrite content in welds of type 21Cr-6Ni-9Mn-0.3N can be estimated better on the basis of Hull's equivalents rather than those of DeLong. A similar observation was made by the author and his co-workers in the case of weld solidification, *i.e.*, that two welds, one alloyed by manganese, the other by nitrogen, behaved more ferritically than could be predicted on the basis of their location on the Schaeffler-DeLong diagram.[16]

The main aim of this work is to study whether these differences in solidification behavior observed in manganese and nitrogen alloyed welds can be explained by selecting suitable coefficients for the chromium and nickel equivalents. For this purpose, about thirty welds alloyed with manganese and/or nitrogen were welded by the gas tungsten arc (GTA) method and analyzed metallographically. The results are compared with those obtained for conventional welds of the types Cr-Ni and Cr-Ni-Mo.

II. EXPERIMENTAL PROCEDURE

The experimental procedure, including welding, sample preparation, metallographic study, and chemical analysis of the weld metals, is exactly as described earlier.[17] Welding was carried out autogeneously by the GTA method on plates of thickness about 8 to 15 mm. The complete welding parameters (Table II) indicate that the welds have partial penetration and an estimated cooling rate of about 300 °C per second at solidification temperatures[18] corresponding to the cooling conditions involved in typical shielded metal arc (SMA) welding with a low heat input.

One experimental improvement is associated with the ferrite content measurements. Earlier only a permeability meter (Fisher's Permascope) was used, but now the Ferrite Numbers (FN) of the welds were determined by a Magne-Gage in accordance with the procedures AWS A 4.2-74 and IIW-Doc. II-904-79. A fair agreement was found between these two methods (Figure 1), allowing comparison of the results with those reported by other authors. The Ferrite Numbers listed in Table III are mean values, the accuracy of which, *i.e.*, the scatter within each weld, is typically as follows:

Range of the FN	Scatter of the FN
0 to 2	0.1 to 0.4
2 to 5	0.2 to 0.5
5 to 10	0.2 to 1.0
10 to 24	0.5 to 2.0

The solidification mode of each weld was evaluated on the basis of the relationship existing between it and the

N. SUUTALA, formerly Research Metallurgist, Laboratory of Physical Metallurgy, University of Oulu, is now Research Engineer, Outokumpu Company, Stainless Steel Division, Tornio, Finland.

Manuscript submitted December 2, 1981.

ISSN 0360-2133/82/1211-2121$00.75/0

Table I. Various Chromium and Nickel Equivalents Developed for the Ferrite Content of Welds,[6,7,8] Ferrite Content of Ingots,[8-11] or Solidification Mode.[12,13]

Chromium Equivalent							
Author	Cr	Mo	Si	Nb	Ti	Constant	Method
Schaeffler	1	1	1.5	0.5	—	—	Weld metals (Ref. 6)
DeLong	1	1	1.5	0.5	—	—	Weld metals (Ref. 7)
Hull†	1	1.21	0.48	0.14	2.20	—	Chill castings (Ref. 8)
Pryce and Andrews*	1	1	3	4Nb′	10Ti′	—	Annealed ingots (Ref. 9)
Guiraldenq	1	2	1.5	1	4	—	Castings (Ref. 10)
Schoefer	1	1	1.5	1	—	−4.99	Castings (Ref. 11)
Hammar and Svensson	1	1.37	1.5	2	3	—	Thermal analysis (Refs. 12, 13)

Nickel Equivalent							
Author	Ni	Mn	C	N	Cu	Constant	Method
Schaeffler	1	0.5	30	—	—	—	Weld metals (Ref. 6)
DeLong	1	0.5	30	30	—	—	Weld metals (Ref. 7)
Hull†	1	0.11Mn-0.0086Mn^2	24.5	18.4	0.44	—	Chill castings (Ref. 8)
Pryce and Andrews	1	0.5	21	11.5	—	—	Annealed ingots (Ref. 9)
Guiraldenq	1	—	30	30	—	—	Castings (Ref. 10)
Schoefer	1	0.5	30	26(N-0.02)	—	+2.77	Castings (Ref. 11)
Hammar and Svensson	1	0.31	22	14.2	1	—	Thermal analysis (Refs. 12, 13)

†Chromium equivalent also includes W, Ta, V, and Al multiplied by the coefficients 0.72, 0.21, 2.27, and 2.48, respectively. Nickel equivalent includes Co, the coefficient for which is 0.41.

*If the Mo content is within 2 to 3 pct, a coefficient of 2 to 4 should be used. The equivalent Nb and Ti contents are $Nb' = Nb - 8\,[(C-0.03) + N]$ and $Ti' = Ti - 4\,[(C-0.03) + N]$.

Table II. Welding Conditions

Filler metal	None
Welding current	190 A†
Pole voltage	14 to 17 V†
Travel speed	8 cm/min
Heat input	17 to 21 kJ/cm†
Arc length	2.0 mm
Electrode	EWTh-2, diameter 2.4 mm, and cone angle 90 deg
Shielding gas	Welding grade Ar, flow 8 l/min (trailing shield, flow 8 l/min)
Torch position	Vertical, orifice diameter 11 mm and distance from the plate 10 mm
Polarity	DC, straight
Welding position	Flat
Technique	Mechanized stringer bead

†These values are valid for the plates of thickness 16 mm. In the case of thinner plates the current was reduced to a value such that the energy equivalent $Q/\sqrt{2s}$ remained unchanged (Q = heat input = current · arc voltage/speed and s = plate thickness).

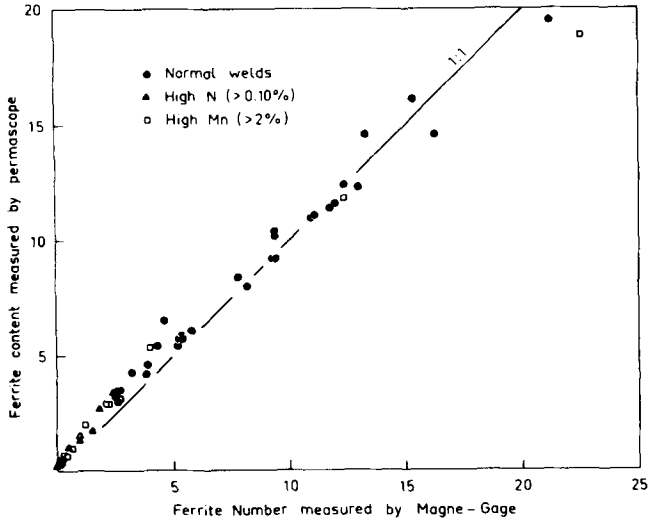

Fig. 1—Relationship between the Ferrite Number measured by a Magne-Gage and the ferrite content measured using a Permascope.

microstructure at room temperature (RT), as described in detail in previous papers.[16,17] Compositional differences in microstructure at RT were studied using an electron probe microanalyzer (EPMA) at 20 kV with a minimum beam diameter (~1 μm). Concentration profiles were determined by an application of the line scanning technique. The specimens were etched slightly before analysis. For quantitative calibration, the average net X-ray intensities obtained from the EPMA were equalized with content values analyzed by spectrometry, followed by a linear approximation.

The chemical compositions of the weld metals deposited, together with their Ferrite Numbers and solidification modes, are given in Table III. The material can be divided into three groups on the basis of the alloying pattern. The first group, the "normal" series, mainly consists of the same Cr-Ni and Cr-Ni-Mo alloyed welds dealt with earlier,[17] the Ferrite Numbers and nitrogen contents of which were nevertheless determined in order to make them intercomparable with those examined here. The other two groups, the N and

Table III. Chemical Compositions of the Weld Metals (Analyzed by Outokumpu Company, Stainless Steel Division). The Ferrite Numbers and Solidification Modes Are Presented in the Last Columns.

C	Si	Mn	P	S	Cr	Ni	Mo	Cu	N	Nb	Ti	FN	Mode	Code
						Normal Series								
0.13	0.29	0.88	0.031	0.013	16.2	11.0	2.3	0.12	0.048	0.00	0.00	0	A	A1
0.039	0.60	1.55	0.031	0.011	18.4	11.7	0.15	0.16	0.043	0.00	0.00	0	A	New1
0.040	0.55	1.4	0.030	0.011	16.9	10.1	0.15	0.16	0.045	0.00	0.00	0	A	New2
0.032	0.80	1.0	0.027	0.006	18.7	16.0	2.3	0.06	0.042	0.00	0.00	0.1	AF	A4
0.024	0.51	1.7	0.031	0.015	16.3	13.1	2.75	0.31	0.029	0.00	0.00	0.2	AF	A6
0.016	0.54	1.7	0.016	0.007	17.3	13.9	2.5	0.02	0.046	0.00	0.00	0.2	AF	New3
0.024	0.86	1.35	0.033	0.008	20.7	17.6	3.3	0.50	0.076	0.00	0.00	0.3	AF	A7
0.024	0.86	1.3	0.040	0.013	20.3	16.3	3.15	0.41	0.070	0.00	0.00	2.0	AF	A8
0.090	0.62	0.87	0.020	0.015	16.9	10.9	2.2	0.09	0.048	0.00	0.00	2.6	AF	A9
0.017	0.76	1.45	0.031	0.014	17.2	12.7	2.65	0.20	0.047	0.00	0.00	2.5	AF	A10
0.080	0.55	0.85	0.017	0.007	17.0	11.4	2.6	0.08	0.060	0.00	0.00	2.7	AF	A11
0.019	0.45	1.35	0.034	0.008	18.4	14.1	3.2	0.20	0.035	0.00	0.00	2.7	AF	A12
0.050	0.36	1.75	0.023	0.010	17.2	11.8	2.8	0.20	0.041	0.00	0.00	3.2	AF	A13
0.030	0.88	1.0	0.023	0.007	17.3	14.5	4.6	0.07	0.059	0.00	0.00	8.2	AF(FA)	A15
0.041	0.60	1.5	0.031	0.011	18.4	10.7	0.15	0.15	0.039	0.00	0.00	1.7	FA(AF)	New4
0.026	0.59	1.2	0.034	0.006	18.8	10.9	0.25	0.15	0.062	0.00	0.00	3.8	FA	B3
0.058	0.50	1.7	0.024	0.019	18.4	13.0	2.9	0.06	0.026	0.00	0.00	4.6	FA	New5
0.062	0.58	1.5	0.046	0.022	17.8	10.3	0.45	0.27	0.008	0.00	0.60	5.2	FA	B5
0.039	0.44	1.5	0.017	0.008	19.2	8.7	0.44	0.10	0.073	0.00	0.00	5.4	FA	B6
0.030	0.19	1.6	0.015	0.004	16.6	10.9	2.4	0.49	0.032	0.00	0.00	5.7	FA	New6
0.042	0.40	1.65	0.016	0.008	17.1	10.8	2.5	0.21	0.058	0.00	0.00	5.8	FA	B7
0.026	0.68	1.6	0.037	0.007	16.8	11.5	2.95	0.18	0.023	0.00	0.00	7.8	FA	B8
0.057	0.66	1.25	0.021	0.007	19.3	9.7	0.03	0.04	0.061	0.61	0.00	9.3	FA	B9
0.046	0.40	0.70	0.018	0.009	18.8	12.2	2.7	0.05	0.041	0.00	0.00	9.4	FA	B10
0.024	0.87	1.35	0.023	0.009	20.7	15.1	2.95	0.26	0.067	0.00	0.00	9.2	FA	B11
0.028	0.87	0.65	0.019	0.008	19.4	9.5	0.09	0.04	0.064	0.00	0.00	9.4	FA	B12
0.030	0.92	0.72	0.016	0.009	18.6	12.3	2.9	0.04	0.041	0.00	0.00	11.0	FA	B13
0.054	0.61	1.2	0.021	0.010	19.6	9.6	0.01	0.08	0.059	0.78	0.00	11.1	FA	B14
0.026	0.88	0.60	0.016	0.008	20.8	10.5	0.03	0.07	0.054	0.00	0.00	11.8	FA	B15
0.032	0.66	1.4	0.032	0.010	18.2	12.0	2.9	0.05	0.051	0.60	0.00	12.0	FA	B16
0.066	0.47	0.81	0.021	0.006	18.2	9.9	2.4	0.10	0.016	0.00	0.00	13.0	FA(F)	B17
0.018	0.93	0.70	0.023	0.009	21.6	11.3	0.01	0.06	0.072	0.30	0.00	13.3	FA	B18
0.086	0.70	1.65	0.023	0.010	25.1	12.5	0.08	0.18	0.092	0.00	0.00	16.3	FA	B19
0.025	1.14	1.35	0.018	0.016	20.3	13.3	2.5	0.09	0.061	0.00	0.00	15.4	FA	B20
0.023	0.93	0.71	0.020	0.008	19.0	10.2	1.5	0.05	0.044	0.00	0.00	9.4	F	C1
0.041	0.37	0.42	0.026	0.021	18.2	9.9	2.4	0.12	0.020	0.00	0.00	12.4	F	C3
0.026	1.00	0.70	0.028	0.016	18.8	10.5	2.5	0.06	0.057	0.35	0.00	15.0	F	C4
0.027	0.68	0.96	0.015	0.012	21.5	12.2	2.3	0.05	0.047	0.00	0.00	21.3	F(FA)	C5
0.084	0.85	0.59	0.019	0.011	20.4	8.9	3.0	0.21	0.056	0.00	0.00	> 24	F	C6
0.027	0.93	1.4	0.028	0.012	19.2	9.0	2.4	0.04	0.053	0.00	0.00	> 24	F	C7
0.045	1.56	0.81	0.022	0.027	21.6	8.5	1.2	0.05	0.054	0.00	0.00	> 24	F	C8

Mn series, comprise the actual new material, also including those "old" welds with a high nitrogen content (>0.10 pct) or high manganese content (>2 pct). More exact descriptions of the N and Mn series would be as follows:

1. The materials in the N series are commercial wrought or cast steels alloyed with nitrogen, corresponding to the types AISI 304N, 304LN, 316N, 316LN, and "317LN".
2. The materials in the Mn series include laboratory-melted and wrought plates alloyed with manganese and nitrogen, corresponding to steels of the AISI 200 series (manufactured by Rautaruukki Oy, Raahe, Finland, and Outokumpu Oy, Tornio, Finland), together with commercial weld filler metals containing 2 to 8 pct Mn. In the case of the filler metals the final GTA welds were made on multipass SMA welds. For the exact procedure, see Reference 17.

Reliable determination of the chemical composition of the weld metal will play an important role, since the composition has an effect on both the solidification mode and the Ferrite Number. Inaccuracies in the concentrations of individual alloying elements will result in inaccuracies in the calculated values for the chromium and nickel equivalents which are of the order of $|\Delta Cr_{eq}| < 0.4$ and $|\Delta Ni_{eq}| < 0.2$ (at carbon contents about 0.15 $|\Delta Ni_{eq}| < 0.8$) at the 95 pct confidence limit.[19] Further analysis showed that there were no marked differences in the compositions of the autogeneous GTA weld and base plate, whereas the nitrogen content of the welds of the N series was a little lower than that of the plates (Figure 2).

III. RESULTS

The macrostructures and microstructures of the welds of the Mn and N series resemble those of the Cr-Ni and Cr-Ni-Mo welds, allowing evaluation of the solidification mode

Table III. Cont. Chemical Compositions of the Weld Metals (Analyzed by Outokumpu Company, Stainless Steel Division). The Ferrite Numbers and Solidification Modes Are Presented in the Last Columns.

C	Si	Mn	P	S	Cr	Ni	Mo	Cu	N	Nb	Ti	FN	Mode	Code
						N Series								
0.012	0.42	1.6	0.022	0.013	18.1	10.5	0.24	0.09	0.150	0.00	0.00	0	A	N1
0.020	0.46	1.5	0.030	0.012	18.2	10.4	0.49	0.26	0.123	0.00	0.00	0.1	AF	N2
0.016	0.35	1.35	0.034	0.001	18.1	10.0	0.34	0.08	0.128	0.00	0.00	1.0	AF(FA)	N3
0.018	0.53	1.7	0.024	0.008	18.0	9.1	0.03	0.02	0.141	0.00	0.00	0.5	FA	N4
0.015	0.50	1.5	0.029	0.003	18.1	9.8	0.14	0.09	0.131	0.00	0.00	1.0	FA	N5
0.020	0.40	1.5	0.027	0.008	18.3	9.1	0.36	0.11	0.139	0.00	0.00	1.5	FA	N6
0.042	0.88	1.25	0.011	0.013	17.5	13.8	2.2	0.06	0.228	0.00	0.00	0	A	N7
0.028	0.58	1.7	0.017	0.004	17.4	13.6	2.7	0.05	0.162	0.00	0.00	0.1	A	N8
0.021	0.54	1.8	0.032	0.005	17.9	13.0	2.7	0.22	0.127	0.00	0.00	0.1	AF	N9
0.026	0.52	1.5	0.032	0.009	17.5	11.3	2.8	0.12	0.133	0.00	0.00	1.8	AF	N10
0.017	0.50	1.4	0.031	0.003	17.6	13.5	4.6	0.19	0.118	0.00	0.00	3.4	AF	N11
0.027	1.15	0.94	0.012	0.010	18.5	14.5	3.2	0.05	0.109	0.00	0.00	3.9	AF	N12
0.021	0.56	1.6	0.035	0.011	17.3	10.5	2.8	0.18	0.127	0.00	0.00	4.3	FA	N13
						Mn Series								
0.038	0.43	5.5	0.011	0.007	17.6	14.6	2.4	0.05	0.039	0.00	0.00	0	A	Mn1
0.034	0.32	3.4	0.015	0.007	18.4	16.0	2.7	0.02	0.046	0.00	0.00	0	A	Mn2
0.060	0.50	5.1	0.021	0.003	24.7	20.1	0.50	0.07	0.063	0.00	0.00	0.2	AF	Mn3
0.11	0.90	9.2	0.023	0.019	18.2	4.7	0.01	0.02	0.325	0.00	0.00	0.1	FA	Mn4
0.16	0.67	8.8	0.032	0.016	18.2	4.6	0.01	2.2	0.242	0.00	0.00	0.2	FA	Mn5
0.18	0.63	9.1	0.033	0.016	19.1	4.8	0.01	1.2	0.245	0.00	0.00	0.2	FA	Mn6
0.070	0.51	8.8	0.022	0.018	18.7	4.8	0.01	0.61	0.359	0.00	0.00	0.2	FA	Mn7
0.13	0.37	6.2	0.011	0.013	17.9	7.9	0.05	0.02	0.076	0.00	0.00	0.3	FA	Mn8
0.065	0.50	8.9	0.029	0.012	16.1	4.3	0.01	1.0	0.196	0.00	0.00	0.4	FA	Mn9
0.036	0.74	8.9	0.021	0.013	16.3	4.3	0.01	1.2	0.192	0.00	0.00	0.7	FA	Mn10
0.096	0.92	7.5	0.018	0.010	17.9	9.8	0.18	0.03	0.036	0.00	0.00	1.2	FA	Mn11
0.086	0.61	7.5	0.036	0.012	16.7	4.2	0.01	1.0	0.120	0.00	0.00	2.1	FA	Mn12
0.11	0.47	8.6	0.040	0.012	15.8	4.4	0.01	1.1	0.037	0.00	0.00	2.2	FA	Mn13
0.030	0.42	8.0	0.030	0.000	17.3	8.9	0.06	0.02	0.037	0.00	0.00	2.7	FA	Mn14
0.064	0.70	8.0	0.029	0.011	17.9	5.6	0.13	0.12	0.153	0.00	0.00	4.0	FA	Mn15
0.046	0.43	2.9	0.022	0.006	23.4	11.4	0.47	0.06	0.055	0.00	0.00	22.6	FA	Mn16
0.060	0.29	2.1	0.026	0.009	16.8	7.9	2.45	0.05	0.037	0.00	0.00	12.4	F	Mn17

Key to the solidification modes: A = austenitic, AF = austenitic-ferritic, FA = ferritic-austenitic, and F = ferritic. The minority mode, if any, is indicated in parentheses.

Note: The Co, Al, V, W, and Ta concentrations needed for the calculation of exact values for Hull's equivalents (Table I) were not obtained by analysis, but these concentrations and consequently also their contributions to the equivalents are so small that they can be disregarded in Figures 4(c) and 5(c). Only the effect of cobalt can be of the same order as that of copper.

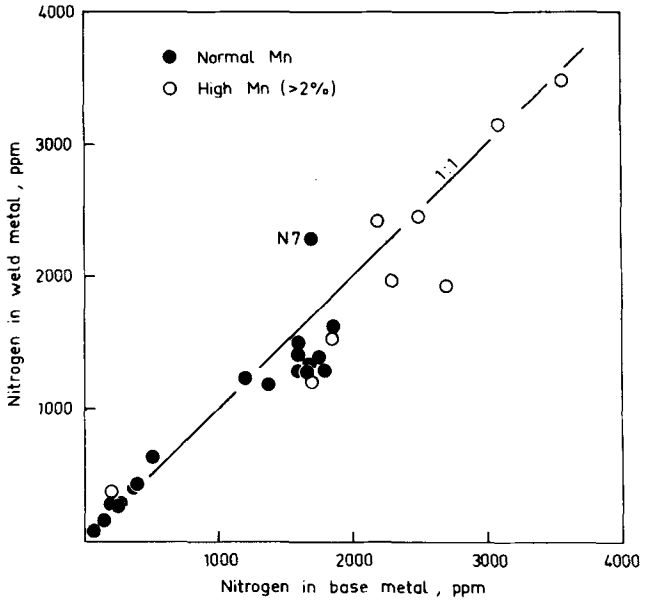

Fig. 2—Dependence of the nitrogen content of the weld metal upon that of the base metal in the autogeneous GTA welding. Weld No. N7 was made on a (inhomogeneous) cast steel.

based on the morphology and location of the ferrite. The most unexpected observation is the fact that welds Numbers Mn3 to Mn8, containing 5 to 8 pct Mn, solidified in a ferritic-austenitic manner even though their Ferrite Numbers were only 0.1 to 0.3 FN (see Table III and Figure 3). Some of the nitrogen-alloyed welds (Numbers N4 to N6) and the normal weld "New 4" also solidified in this manner in spite of their low FN (0.5 to 1.7). Although it is difficult to distinguish the austenitic-ferritic and ferritic-austenitic solidification mode at so low ferrite levels, erroneous interpretations can be avoided, if the examination is performed using both low and high magnifications under a light microscope. Low magnifications ensure that the typical features of the corresponding microstructures, the regularity and irregularity, respectively, can be found.[16] In the particular case of Figure 3, for instance, the ferrite (and its traces) is located at the dendrite axis, which is a proof of the ferritic-austenitic solidification and almost complete transformation from ferrite to austenite. In the welds solidified austenitic-ferritically the retained ferrite is located in interdendritic regions, and the structure is more regular being due to the well-retained solidification substructure (to the slow diffusion rate in the austenite).[17]

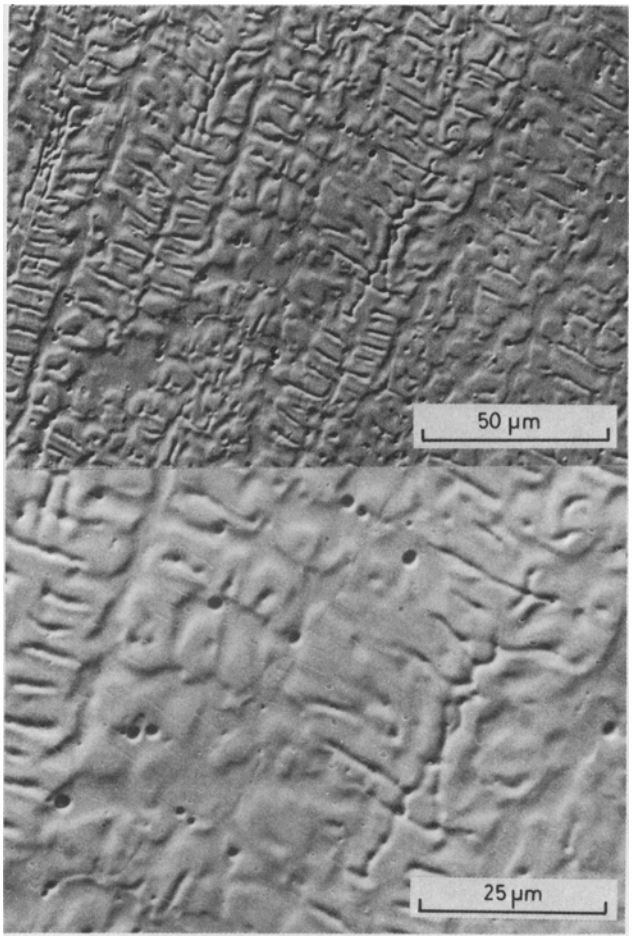

Fig. 3 — Microstructures in weld No. Mn5 (SEM micrographs). The location of traces of the ferrite retained at the dendrite axis is proof of ferritic-austenitic solidification (see Fig. 6). The specimen was polished electrolytically in the solution CH_3OH + 30 pct HNO_3 (T = −25 °C, U = 12 V) and etched electrolytically in 10N NaOH (U = 2 to 3 V).

In the following the results are discussed in terms of three different chromium and nickel equivalents acquired from the literature, referred to here as DeLong's, Hammar's, and Hull's equivalents (see Table I). DeLong[7] and Hull[8] diagrams were developed to predict retained ferrite in welds and in small (~20 g) chill castings as measured by a Magne-Gage. The thermal histories of the samples used for these diagrams were dissimilar, and thus the coefficients in chromium and nickel equivalents can differ. Hammar's equivalents were determined by means of the thermal analysis at a cooling rate about 20 °C per minute,[12] which is much lower than in arc welding. However, they are the only equivalents devised for the solidification mode.

A. *Ferrite Number*

The correlation between composition and Ferrite Number is presented in Figure 4. As seen in Figure 4(a), the DeLong diagram predicts the FN well in normal and nitrogen-alloyed welds and satisfactorily in welds Numbers Mn2, Mn16, and Mn17, which contain 2 to 3.5 pct Mn. On the other hand, it gives obviously too low values for welds Numbers Mn3 to Mn15, which contain 5 to 8 pct Mn.

The equivalents developed by Hammar and Svensson are devised for the solidification mode, and there is no ready diagram for the FN in welds or ingots based on the use of these equivalents. The isoferrite lines imagined on the basis of the FN values measured here (Figure 4(b)) have a somewhat higher location than the lines "0 pct ferrite" and "5 pct ferrite" which describe the equilibrium content in small castings annealed eight hours at 1200 °C and quenched.[12] This difference is indicative of a decrease in ferrite content during such an annealing, in particular, in a composition field in which the sum Cr_{eq} + Ni_{eq} is low. Additionally, as seen in Figure 4(b), the welds which are highly alloyed with manganese seem to behave in a more ferritic manner than their location on the Cr_{eq}-Ni_{eq} plot would presuppose.

The Hull diagram also predicts the FN correctly in manganese-alloyed welds (Figure 4(c)), but its accuracy in the case of normal and nitrogen-alloyed welds is somewhat poorer than that of the DeLong diagram.

B. *Solidification Mode*

The correlation between the composition and solidification mode (Figure 5) is better than that between the composition and Ferrite Number (Figure 4). As far as normal and nitrogen-alloyed welds are concerned, the solidification modes have well-defined fields on the Cr_{eq}-Ni_{eq} plots. The locations of these borderlines and the scatter associated with them is to a certain extent dependent on the equivalents used. DeLong's equivalents produce the greatest scatter (Figure 5(a)) and Hammar's equivalents the least (Figure 5(b)). When using Hammar's equivalents the demarcation between the austenitic-ferritic and ferritic-austenitic solidification modes corresponds to values of 1.52 ± 0.01 for the ratio Cr_{eq}/Ni_{eq}, and the demarcation between the ferritic-austenitic and single-phase ferritic solidification modes to values of 1.90 ± 0.04. The poorer accuracy in the latter case is at least partly due to the smaller number of data points in the vicinity of this borderline.

Welds Numbers Mn2, Mn16, and Mn17, containing 2 to 3.5 pct Mn, solidified in the same manner as those with normal contents of 1 to 2 pct Mn (see Figure 5), whereas those containing 5 to 8 pct Mn behaved more ferritically than the other welds regardless of the equivalents used. Hull's equivalents nevertheless produce a tolerable agreement when comparing the solidification mode in these welds with that found in other welds (Figure 5(c)).

C. *Segregation and Partitioning*

Concentration profiles were determined for some of the alloying elements in welds Numbers N4, Mn5, Mn13, and Mn15 and also for weld Number B3 for the sake of the comparison. The solidification mode in these welds was ferritic-austenitic and their Ferrite Numbers varied from 0.2 to 4 FN. Typical profiles in the case of two manganese-alloyed welds (Numbers Mn5 and Mn15) are presented in Figure 6. They indicate that the interdendritic regions are depleted in Cr and enriched in Ni and Mn, and thus confirm the ferritic-austenitic solidification, which is characterized by the description "ungleichsinnige Seigerung" of chromium and nickel.[16,20] Manganese segregates in the same manner as nickel. During the transformation from ferrite to austenite, the ferrite becomes poorer in Ni and Mn and richer in Cr, as

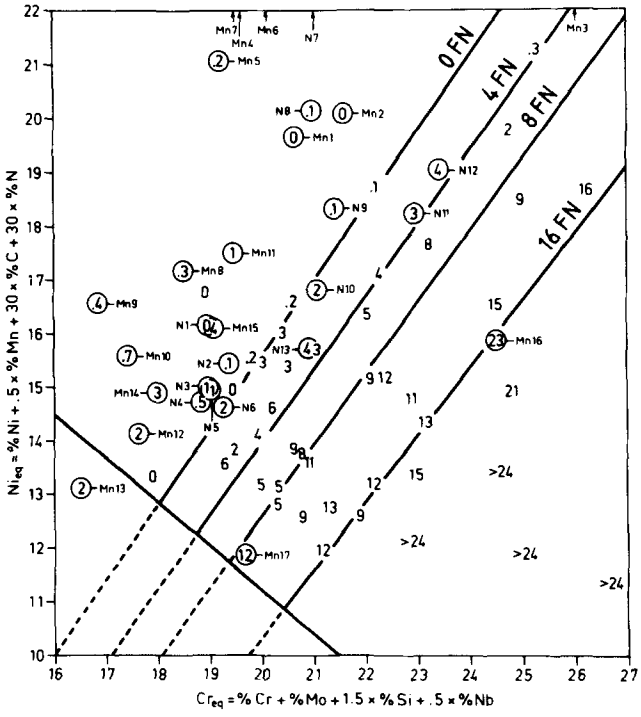

(a)

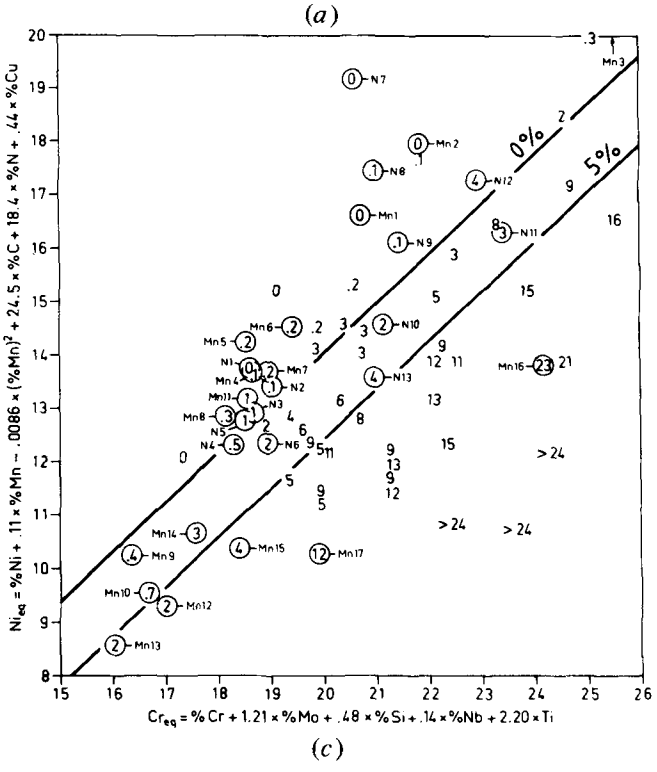

(c)

may be concluded from the distinct minima and maxima corresponding to the retained ferrite particles (Figure 6(a)). The partitioning of manganese is quite neutral as compared with that of nickel, however, which appears especially well in Figure 6(b). In this figure the concentration profile of chromium is also surprisingly flat.

Compositional variations in the as-welded structure are described more quantitatively* in Table IV, which shows

*Note: The electron probe beam diameter (~1 μm) is one order smaller than the segregation distance, but of the same order as the thickness of the delta ferrite particles. Consequently, the estimated values for the segregation ratio are unaffected, but the true partitioning is more extensive than shown in Table IV. The values for the welds are intercomparable, however.

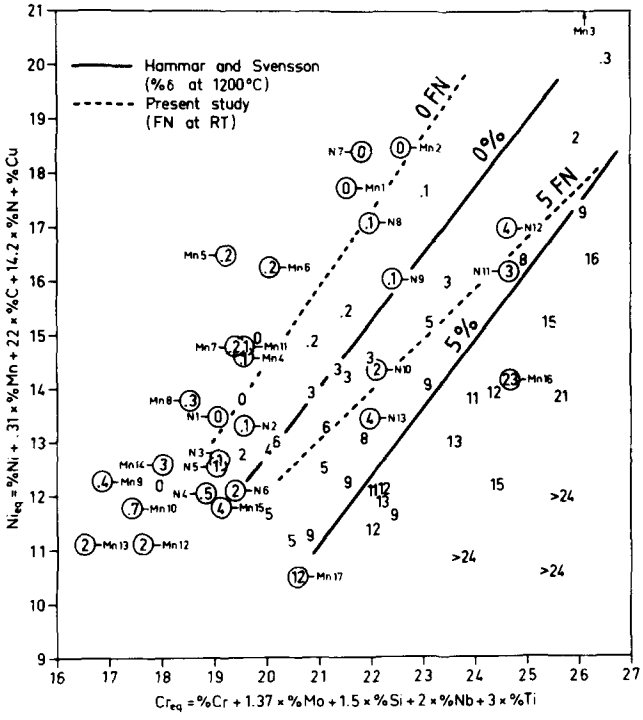

(b)

Fig. 4—Relationship between the composition and Ferrite Number, in terms of (*a*) DeLong's equivalents, (*b*) Hammar's equivalents, and (*c*) Hull's equivalents (see footnote to Table III). Circled values are the Ferrite Numbers measured from the welds of N and Mn series; uncircled values are from normal welds.

that neither the increase in manganese content from 1.5 to 8 pct nor the nitrogen alloying seems to contribute at all markedly to the segregation and partition ratios for chromium, nickel, and manganese. Incidentally, copper segregates in the same manner as nickel in weld Number Mn5 (see Figure 6 and Table IV).

Table IV. Measured Values for Segregation Ratio *S*, and Partition Ratio P_D Characterizing Compositional Variations in the Welds Solidified in Ferritic-Austenitic Manner

Weld Number	Type	Cr	Ni	Mn	Cu	Fe
	Segregation Ratio *S*					
B3	Cr-Ni	0.95	1.28	1.24	NM	0.96
N4	Cr-Ni-N	1.00	1.24	1.22	NM	0.96
Mn13	Cr-Ni-Mn	0.94	1.30	1.16	NM	NM
Mn15	Cr-Ni-Mn-N	0.96	1.23	1.14	NM	0.97
Mn5	Cr-Ni-Mn-Cu-N	1.02	1.30	1.22	1.56	0.92
	Partition Ratio P_D					
B3	Cr-Ni	1.08	0.86	1.0	NM	1.0
N4	Cr-Ni-N	1.10	0.82	0.98	NM	1.0
Mn13	Cr-Ni-Mn	1.08	0.83	0.97	NM	NM
Mn15	Cr-Ni-Mn-N	1.03	0.81	0.98	NM	1.0
Mn5	Cr-Ni-Mn-Cu-N	1.07	0.84	0.95	1.0	1.0

NM = not measured

Segregation ratio *S* = ratio of the concentration of an element in the interdendritic areas to that at the center of the dendrites.

Partition ratio P_D = ratio of the concentration of an element in dendritic ferrite to that in adjacent austenite.

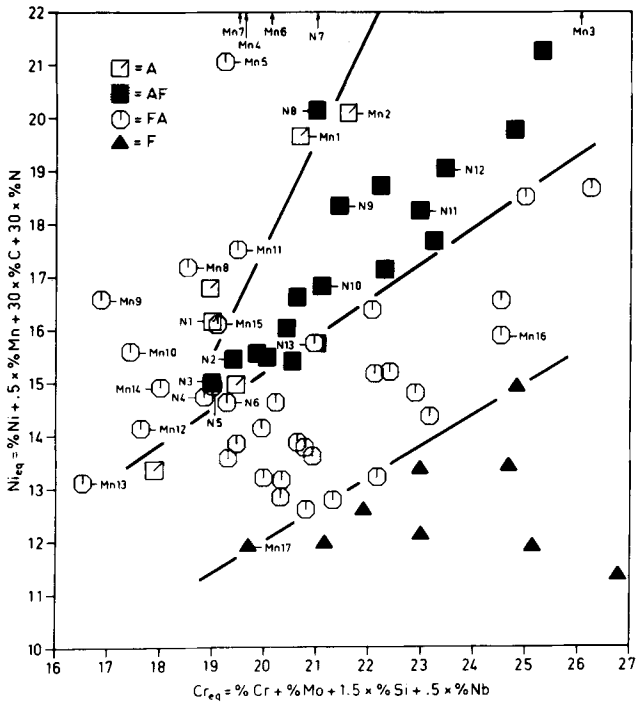

(a)

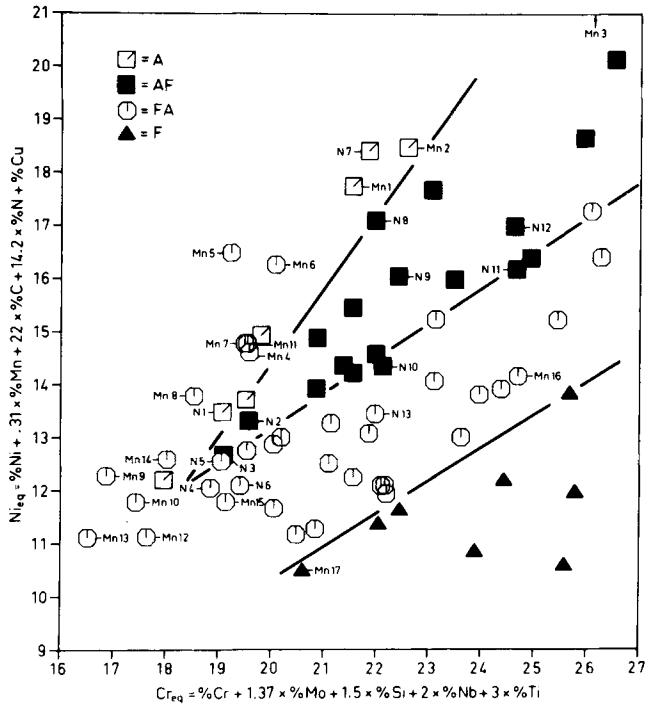

(b)

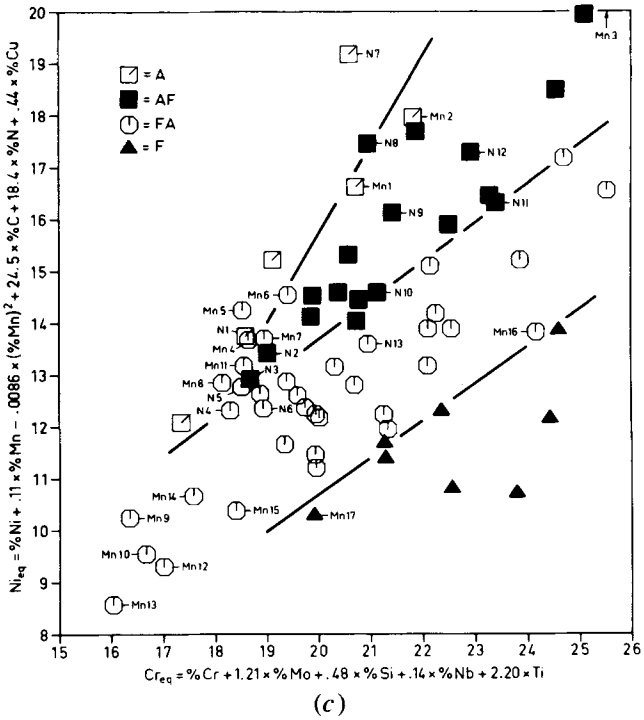

(c)

Fig. 5—Relationship between the composition and solidification mode, in terms of (*a*) DeLong's equivalents, (*b*) Hammar's equivalents, and (*c*) Hull's equivalents (see footnote to Table III).

IV. DISCUSSION

A. *Equivalent Problem*

The results of this study confirm the fact that the effect of composition on the solidification mode and Ferrite Number in austenitic stainless steel welds can be described adequately using chromium and nickel equivalents, although different equivalents are needed for this purpose. The statistical data are too restricted to allow new equivalents to be developed, but some remarks can be still made on the nature of the "best" coefficients.

The solidification mode in the welds of the AISI/AWS 300 series and their nitrogen-alloyed modifications can be predicted excellently using Hammar's equivalents (Figure 5(b)), the transition from primary austenitic to primary ferritic solidification corresponding to a value of 1.52 for the ratio Cr_{eq}/Ni_{eq}. The scatter is very slight compared with the accuracy of the composition determinations. However, these equivalents may be uncertain in the welds which contain exceptional amounts of copper, niobium, titanium, and perhaps silicon. This is due to the fact that the contents of these elements did not vary sufficiently in this material nor in that of Hammar and Svensson,[12] but they are drawn from the other equivalents aimed at the ferrite content as done in Reference 13.

The Ferrite Number in normal and nitrogen-alloyed welds can be predicted fairly well from a conventional Schaeffler-DeLong diagram (Figure 4(a)). The accuracy of the results presented in Figure 4(a) is 3 FN, which is the same as the accuracy of this diagram as stated by DeLong[21] and Kotecki.[22]

At manganese contents of 5 to 8 pct Hull's equivalents give the most satisfactory correlation between the composition and solidification mode or Ferrite Number (Figures 4(c) and 5(c)), if a good agreement is to be maintained with other austenitic stainless welds. The scatter is greater in this case than in normal welds, however. Mathematical conformity could obviously be achieved by the selection of suitable coefficients for the nickel equivalent. For instance, if

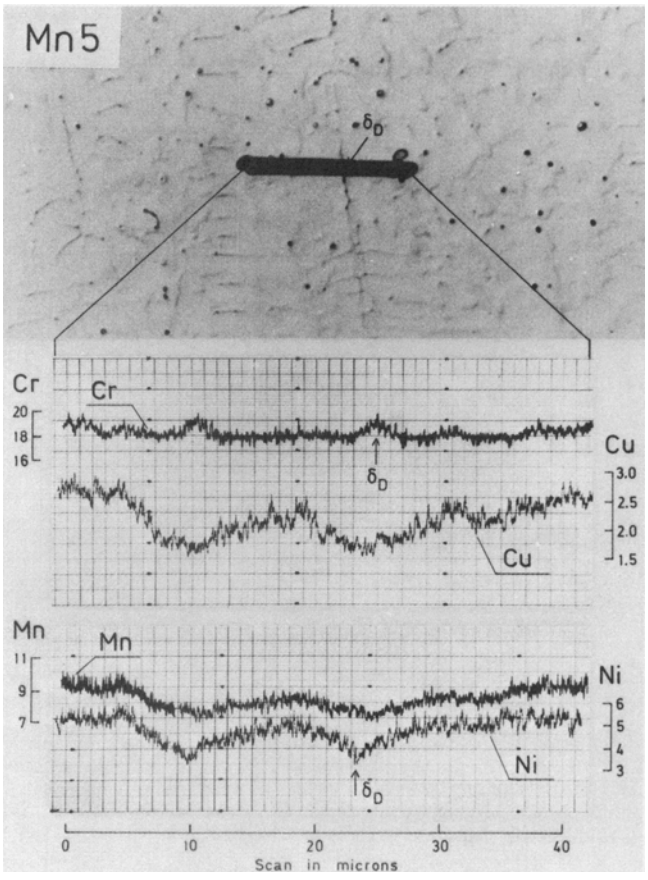

(a)

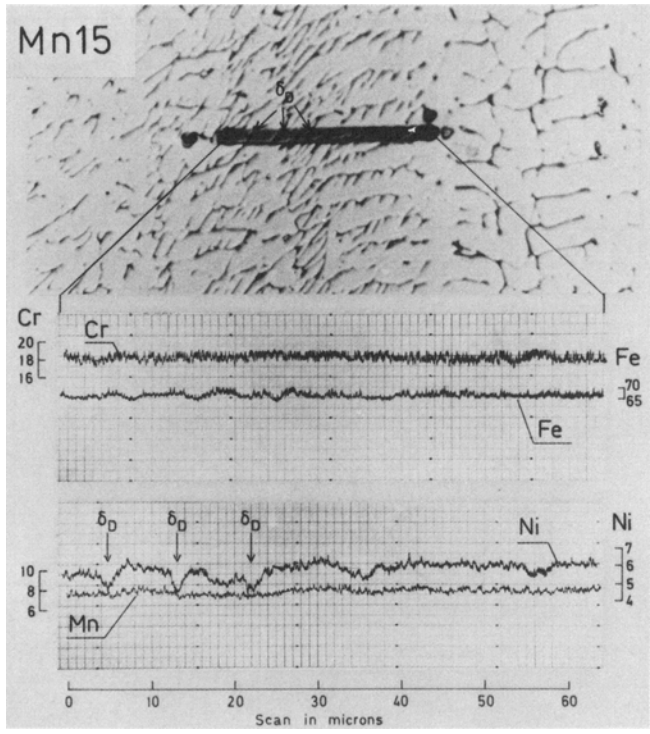

(b)

Fig. 6—Concentration profiles of some alloying elements in weld Nos. Mn5 and Mn15. The retained ferrite is labeled by δ_D. For the etching method, see Fig. 3.

Hammar's coefficients of 22 for carbon and 14.2 for nitrogen are used instead of the values 24.5 and 18.4 in Hull's equivalents, the scatter associated with the location of the borderline between primary austenitic and ferritic solidification can be reduced. Physical interpretation of the effect of manganese is difficult, however.

B. *Effect of Manganese*

The role of manganese in austenitic stainless steels is dualistic and complicated. At low concentrations it is an "austenitizer." At concentrations of 5 to 8 pct manganese behaves almost as a "ferritizer" or at least its austenite-favoring effect on the solidification mode is insignificant, which corresponds to, *e.g.*, Hull's statement of its effect on the ferrite content.[8] At subsolidus temperatures manganese is a weak austenitizer, as concluded from its partitioning behavior, *i.e.*, from the manganese depletion of the retained ferrite.

In ferritic-austenitic solidification manganese segregates in the same way and as strongly as nickel (Table IV). Its enrichment in the interdendritic regions indicates that its equilibrium distribution coefficient between the liquid and ferrite (austenite) is < 1. This is true at both normal and high concentrations. This segregation behavior does not solve the problem of its austenite or ferrite-favoring effect, however, since the corresponding coefficient for silicon, for instance, which is generally assumed to be a ferritizer, is also < 1 and of the same order as for manganese in normal austenitic stainless steels.[23] The partitioning of manganese instead suggest that manganese favors austenite at subsolidus temperatures. Since its partitioning is less extensive than that of nickel, manganese is a weaker austenitizer. In this respect the results of this study agree well with those obtained from annealing experiments at temperatures of 1050 to 1350 °C.[10,24,25] Partition ratios of 0.80 to 0.97 were measured for manganese at concentration of 1 to 8 pct in these studies, and the corresponding values for nickel and chromium varied in the ranges 0.58 to 0.71 and 1.0 to 1.33, respectively.

In addition to the possible temperature-dependence, a composition-dependence is perhaps also involved in the role of manganese. According to Guiraldenq,[26] manganese has a very low nickel equivalent effect when nickel is present in the alloy, whereas without nickel it has a real ferritic effect, which increases with temperature. Another explanation for the low nickel equivalent effect of manganese is thought to be that manganese forms nitrides in the melt before solidification (or binds free nitrogen in some other way), and thus reduces the effective nitrogen content. This explanation does not seem credible, however, since the welds of the Mn series containing variable amounts of manganese, nitrogen, and carbon behave similarly, and since nitrogen does not seem to have a marked effect on the segregation or partitioning of manganese (see Table IV). There is an interaction between manganese and nitrogen, however, which appears in Figure 2 as an unchanged nitrogen content in

weld metals highly alloyed with manganese. The slight partitioning of chromium and manganese in the weld Mn15 (Figure 6(b)) may also point to less-understood interactions between alloying elements in these alloys, since in normal welds the partitioning of chromium between austenite and lathy ferrite is clear.[16]

C. *Effect of Nitrogen*

The role of nitrogen in austenitic stainless steels is simpler than that of manganese, provided that one excludes its possible interactions with stabilizing elements and with manganese at high concentrations. In fact, nitrogen and carbon have quite similar effects on the solidification mode and Ferrite Number. The austenite-favoring effect of nitrogen strengthens with decreasing temperature as that of carbon, since it contributes to the solidification mode with a coefficient 14.2 (Hammar's value) and to the FN with a coefficient 18.4 to 30 (Hull's and DeLong's values), while the respective values for carbon are 22 and 24.5 to 30.

The temperature dependency of the effects of nitrogen and carbon, *i.e.*, the different coefficients in the nickel equivalents in respect of the solidification mode and FN, may be directly associated with their differing effects on the phase equilibria at different temperatures. This statement is supported by the results of annealing experiments, in which quite different coefficients are obtained for carbon and nitrogen depending on temperature in the range 1100 to 1300 °C.[27] This temperature dependency may also partly be due to kinetic factors, *i.e.*, to the more rapid diffusion of these interstitial elements, which allows a more rapid phase transformation from ferrite to austenite during continuous cooling and thus results in a lower FN.

D. *Some Practical Aspects*

The solidification mode can be predicted well using diagrams based on chromium and nickel equivalents (Figure 5). This information is of great practical importance, since welds solidifying primarily as austenite are prone to solidification cracking[28,29] and since the location of this borderline is only to a minor extent dependent on the solidification conditions.[30] In fact, its position is surprisingly close to the Fe-Cr-Ni ternary eutectic liquidus as noted earlier.[16,17]

The boundaries of the fields of the different solidification modes cross the constant ferrite lines independently of the equivalents used (see Figures 4 and 5). Consequently, the modes cannot be identified uniquely on the basis of the Ferrite Number. Under the welding conditions of this study, for instance, the transition from primary austenitic to primary ferritic solidification corresponds to values 3 to 5 FN for Type 316 materials, while the values 0.5 to 1 FN are valid for Type 304N materials (see Table III).

As is generally known, welds highly alloyed with manganese are resistant to solidification cracking in spite of their entirely or almost entirely austenitic microstructure under as-welded conditions. In the case of type 18Cr-8Mn-6Ni the resistance may be due to ferritic-austenitic solidification, which is possible in these welds at ferrite levels of 0.1 to 0.3 FN (see Table III). Manganese must also have some individual effects, however, for welds of type 20Cr-25Ni-5Mn, which will certainly solidify austenitically, are also resistant.[3,4,5] On the other hand, there are some observations that ingots containing only 0.15 pct Mn possess a poor hot ductility in spite of their ferritic-austenitic solidification.[31]

The nitrogen alloyed grades constitute suitable materials for cryogenic applications, but several factors affecting low-temperature toughness must be taken into account when selecting filler metals for these.[32] Weld deposits which solidify as primary delta ferrite resist microfissuring and appear to be immune to intergranular embrittlement at low temperatures under ordinary welding conditions. It is necessary to minimize the ferrite content, however, and on the other hand filler metals having the lowest attainable nitrogen content are recommended.[32,33] According to the present results, the first two requirements are satisfied if the ratio Cr_{eq}/Ni_{eq} is sufficiently high and the sum $Cr_{eq} + Ni_{eq}$ is simultaneously sufficiently low (see Figures 4 and 5). One detail shows that in autogeneous GTA welding the nitrogen content remains relatively unchanged, particularly if a higher amount of manganese is present simultaneously (Figure 2).

V. SUMMARY AND CONCLUSIONS

The solidification and Ferrite Number are studied in autogeneous gas tungsten arc (GTA) welds on austenitic stainless steel plates alloyed with manganese and/or nitrogen, and the results are compared with those obtained for normal welds of the AISI/AWS 300 series using three different chromium and nickel equivalents:

DeLong

$$\begin{cases} Cr_{eq} = \text{pct Cr} + \text{pct Mo} + 1.5\ \text{pct Si} + 0.5\ \text{pct Nb} \\ Ni_{eq} = \text{pct Ni} + 0.5\ \text{pct Mn} + 30\ \text{pct C} + 30\ \text{pct N} \end{cases}$$

Hammar

$$\begin{cases} Cr_{eq} = \text{pct Cr} + 1.37\ \text{pct Mo} + 1.5\ \text{pct Si} + 2\ \text{pct Nb} \\ \qquad + 3\ \text{pct Ti} \\ Ni_{eq} = \text{pct Ni} + 0.31\ \text{pct Mn} + 22\ \text{pct C} + 14.2\ \text{pct N} \\ \qquad + \text{pct Cu} \end{cases}$$

Hull

$$\begin{cases} Cr_{eq} = \text{pct Cr} + 1.21\ \text{pct Mo} + 0.48\ \text{pct Si} \\ \qquad + 0.14\ \text{pct Nb} + 2.20\ \text{pct Ti} + 0.72\ \text{pct W} \\ \qquad + 0.21\ \text{pct Ta} + 2.27\ \text{pct V} + 2.48\ \text{pct Al} \\ Ni_{eq} = \text{pct Ni} + 0.11\ \text{pct Mn} - 0.0086\ (\text{pct Mn})^2 \\ \qquad + 24.5\ \text{pct C} + 18.4\ \text{pct N} + 0.44\ \text{pct Cu} \\ \qquad + 0.41\ \text{pct Co} \end{cases}$$

This comparison allows the following conclusions to be reached:

1. In welds of the AISI/AWS 300 series and their nitrogen-alloyed modifications the solidification mode can be best described using Hammar's equivalents. The Ferrite Number in these welds can be predicted fairly well on the basis of the conventional Schaeffler-DeLong diagram.
2. DeLong's and Hammar's equivalents are invalid at high manganese concentrations (5 to 8 pct). In this case Hull's equivalents give a tolerable correlation between the composition and solidification mode and a fair correlation between the composition and Ferrite Number.
3. The role of manganese is complicated. At normal content values (1 to 2 pct) it is an austenitizer, but at high values (5 to 8 pct) it behaves as "ferritizer" or a weak austenitizer. It resembles nickel in its segregation and partitioning, independent of the content concerned.

4. Nitrogen is indisputably an austenitizer, and its relative austenite-favoring effect increases with decreasing temperature, as does that of carbon, as concluded from the different coefficients in the nickel equivalent needed for the solidification mode and the FN.

ACKNOWLEDGMENTS

The author wishes to thank the various Finnish and Swedish industrial companies concerned for supplying materials. He would also thank Mr. P. Suvanto and the staff of the analytical laboratory of Outokumpu Oy, Stainless Steel Division, for data concerning the composition determinations, and Mr. J. Miettinen for help in the computer work. The financial support provided by the Foundation of Outokumpu Oy, Foundation for the Advancement of Technology and the Academy of Finland, is gratefully acknowledged. Finally, the author wishes to thank Mr. M. Hicks for revising the English language of the manuscript.

REFERENCES

1. J. Degerbeck: *Werkst. Korros.*, 1978, vol. 29, pp. 179-88.
2. A. Garner: *Corrosion*, 1981, vol. 37, pp. 178-84.
3. J. Honeycombe and T. G. Gooch: *Met. Con. and Brit. Weld. J.*, 1972, vol. 4, pp. 456-60.
4. A. Backman and B. Lundqvist: *Weld. J.*, 1977, vol. 56, pp. 23s-28s.
5. C. D. Lundin, C.-P. D. Chou, and C. J. Sullivan: *Weld. J.*, 1980, vol. 59, pp. 226s-32s.
6. A. L. Schaeffler: *Met. Progr.*, 1949, vol. 56, pp. 680 and 680 B.
7. W. T. DeLong, G. A. Ostrom, and E. R. Szumachowski: *Weld. J.*, 1956, vol. 35, pp. 526s-32s.
8. F. C. Hull: *Weld. J.*, 1973, vol. 52, pp. 193s-203s.
9. L. Pryce and K. W. Andrews: *JISI*, 1960, vol. 198, pp. 415-17.
10. P. Guiraldenq: *Mém. Sci. Rev. Mét.*, 1967, vol. 64, pp. 907-38.
11. E. A. Schoefer: *Met. Prog., Databook 1977*, Mid-June 1977, p. 51.
12. Ö. Hammar and U. Svensson: *Solidification and Casting of Metals*, The Metals Society, London, 1979, pp. 401-10.
13. A guide to the solidification of steels, Jernkontoret, Stockholm, 1977.
14. J. Hochmann: *Materiaux et Techniques*, December 1977, pp. 69-87.
15. J. A. Brooks: *Weld. J.*, 1975, vol. 54, pp. 189s-95s.
16. N. Suutala, T. Takalo, and T. Moisio: *Metall. Trans. A*, 1980, vol. 11A, pp. 717-25.
17. T. Takalo, N. Suutala, and T. Moisio: *Metall. Trans. A*, 1979, vol. 10A, pp. 1173-80.
18. D. Rosenthal: *Trans. ASME*, 1946, vol. 68, pp. 849-66.
19. E. Kuula: Outokumpu Oy, Tornio, private communication, September 1981.
20. V. Siegel and M. Günzel: *Neue Hütte*, part I, 1973, vol. 18, pp. 422-29; *Neue Hütte*, part II, 1973, vol. 18, pp. 599-602.
21. W. T. DeLong: *Weld. J.*, 1974, vol. 53, pp. 273s-86s.
22. D. J. Kotecki: *Weld. J.*, 1978, vol. 57, pp. 109s-17s.
23. M. Suzuki, T. Asano, T. Umeda, and Y. Kimura: *Trans. ISIJ*, 1981, vol. 21, p. B-64.
24. R. Nakagawa, Y. Otoguro, and Y. Kawabe: *Mém. Sci. Rev. Mét.*, 1966, vol. 63, pp. 906-09.
25. C. Liang-shi and F. Tie-ying: *Acta Met. Sinica*, 1978, vol. 14, pp. 153-64.
26. P. Guiraldenq: Solid-solid Phase Transformations, ASM, in press.
27. Ö. Hammar: *Sandvik AB*, Sandviken, private communication, March 1980.
28. H. Thier: *DVS-Berichte*, Band 41, pp. 100-06, DVS GmbH, Düsseldorf, 1976.
29. V. Kujanpää, N. Suutala, T. Takalo, and T. Moisio: *Met. Con.*, 1980, vol. 12, pp. 282-85.
30. N. Suutala and T. Moisio: *Solidification Technology in the Foundry and Casthouse*, The Metals Society, London, in press.
31. S. Malm: Report No. D 268, Jernkontoret, Stockholm, January 1979.
32. C. E. Witherell: *Weld. J.*, 1980, vol. 59, pp. 326s-42s.
33. E. R. Szumachowski and H. F. Read: *Weld. J.*, 1979, vol. 58, pp. 34s-44s.